

Coronavirus mRNA Transcription: UV Light Transcriptional Mapping Studies Suggest an Early Requirement for a Genomic-Length Template

KYOKO YOKOMORI, LISA R. BANNER,[†] AND MICHAEL M. C. LAI*

*Howard Hughes Medical Institute and Department of Microbiology, School of Medicine,
University of Southern California, Los Angeles, California 90033-1054*

Received 2 December 1991/Accepted 20 April 1992

Mouse hepatitis virus (MHV) synthesizes seven to eight mRNAs, each of which contains a leader RNA derived from the 5' end of the genome. To understand the mechanism of synthesis of these mRNAs, we studied how the synthesis of each mRNA was affected by UV irradiation at different time points after infection. When MHV-infected cells were UV irradiated at a late time in infection (5 h postinfection), the syntheses of the various mRNAs were inhibited to different extents in proportion to the sizes of the mRNAs. Analysis of the UV inactivation kinetics revealed that the UV target size of each mRNA was equivalent to its own physical size. In contrast, when cells were irradiated at 2.5 or 3 h postinfection, there appeared to be two different kinetics of inhibition of mRNA synthesis: the synthesis of every mRNA was inhibited to the same extent by a small UV dose, but the remaining mRNA synthesis was inhibited by additional UV doses at different rates for different mRNAs in proportion to RNA size. The analysis of the UV inactivation kinetics indicated that the UV target sizes for the majority of mRNAs were equivalent to that of the genomic-size RNA early in the infection. These results suggest that MHV mRNA synthesis requires the presence of a genomic-length RNA template at least early in the infection. In contrast, later in the infection, the sizes of the templates used for mRNA synthesis were equivalent to the physical sizes of each mRNA. The possibility that the genomic-length RNA required early in the infection was used only for the synthesis of a polymerase rather than as a template for mRNA synthesis was ruled out by examining the UV sensitivity of a defective interfering (DI) RNA. We found that the UV target size for the DI RNA early in infection was much smaller than that for mRNAs 6 and 7, which are approximately equal to or smaller in size than the DI RNA. This result indicates that even though DI RNA and viral mRNAs are synthesized by the same polymerase, mRNAs are synthesized from a larger (genomic-length) template. We conclude that a genomic-length RNA template is required for MHV subgenomic mRNA synthesis at least early in infection. Several transcription models are proposed.

Mouse hepatitis virus (MHV), a member of the family *Coronaviridae*, contains a single-stranded, positive-sense RNA genome of 31 kb (15, 26). It contains seven or eight genes, each of which is expressed through a subgenomic mRNA (except for the 5'-most gene, gene 1, which is expressed through the genome-size RNA) (11). These mRNAs, termed mRNAs 1 through 7, have a 3'-coterminal nested-set structure; i.e., the sequence of each mRNA starts from the 3' end of the genome, extending for various distances into the 5' end, and is contained entirely within the next-larger mRNA (13, 17). Thus, each mRNA is structurally polycistronic; however, all of them are functionally monocistronic, since only their 5'-most open reading frames, which contain the unique sequence not overlapping with the sequence of the next-smaller mRNA, are translated (16). These mRNAs have another unique feature: each mRNA contains a leader sequence of approximately 70 nucleotides, which is derived from the 5' end of the genome (12, 33). This leader sequence is present only at the 5' end of the genomic RNA; however, the sequence at the 3' end of the leader is homologous, to various extents, with sequences preceding each gene (32). These intergenic regions are the fusion sites between the leader RNA and the rest of sequences in each

mRNA and represent the transcription initiation sites for each mRNA.

There have been considerable controversies concerning the mechanism of transcription of coronavirus subgenomic mRNAs. Because of the discontinuous nature of the leader and coding sequences in each mRNA, they must be synthesized by a discontinuous transcription mechanism or by a posttranscriptional splicing event. We previously proposed a leader-primed transcription mechanism, in which a leader RNA is synthesized from a full-length negative-stranded RNA template, dissociates from the template, and then rejoins the template RNA at the downstream intergenic sites to serve as a primer for transcription (4, 11). This transcription model is supported by several pieces of evidence, including the following: (i) free leader RNA species have been detected in MHV-infected cells (5); (ii) a temperature-sensitive mutant which synthesizes only the leader RNA, not mRNAs, at the nonpermissive temperature has been isolated (5); (iii) during mixed infection, the leader RNA can be freely exchanged between two MHVs, suggesting that the leader RNA and mRNAs are two independent transcriptional units (20, 24); (iv) the leader fusion sites on the mRNAs are heterogeneous, suggesting an imprecise leader fusion event (23); (v) a leader-containing RNA fragment derived from the 5' end of the MHV genome can be used for mRNA synthesis in an in vitro transcription system, mimicking in vivo MHV mRNA synthesis (2); and (vi) some mRNAs, e.g., mRNA 2-1, are synthesized only by viruses

* Corresponding author.

[†] Present address: Division of Biology, California Institute of Technology, Pasadena, CA 91125.

containing two copies of a UCUAA pentanucleotide sequence in the leader RNA, but some other mRNAs, e.g., mRNA 3-1, can be synthesized only by viruses with three UCUAA repeats, indicating that the transcriptional initiation of mRNAs is regulated by the leader sequence (14, 19, 31).

However, the recent detection of subgenomic negative-stranded RNAs and replicative intermediate RNAs in coronavirus-infected cells suggested an alternative mechanism of mRNA transcription (9, 28–30). These data suggest that subgenomic mRNAs may be transcribed directly from the subgenomic negative-stranded RNAs. In this model, the subgenomic negative-stranded RNA could be generated by discontinuous transcription occurring during negative-stranded RNA synthesis or by an unconventional RNA splicing mechanism (28). Another possibility is that subgenomic negative-stranded RNAs are transcribed directly from the subgenomic mRNAs nonspecifically packaged into the virion (29). It was proposed that coronaviruses could behave like a virus with a segmented RNA genome, using these subgenomic mRNAs for the replication of viral genetic material (29). Although these models are not necessarily mutually exclusive, their mechanisms of transcription are substantially different from the leader-primed transcription mechanism proposed previously.

One way to determine the mode of RNA transcription is by determining the target sizes of the subgenomic mRNAs by UV inactivation. This approach has been used for deciphering the mechanism of RNA synthesis of vesicular stomatitis virus, Sendai virus, and other viruses (1, 3, 7). Previous UV transcriptional mapping studies performed on coronaviruses, including MHV and avian infectious bronchitis virus, indicated that the UV target sizes of coronavirus mRNAs are the same as their physical sizes (10, 34). This result was used to propose the leader-primed transcription mechanism (4, 11). However, in these studies, UV irradiation was performed late in coronavirus replication. In view of the recent detection of subgenomic negative-stranded RNAs and replicative intermediates, these results were not unexpected, but they did not reveal how the subgenomic negative-stranded RNAs were synthesized. In this paper, we report a UV transcriptional mapping study performed early in the viral replication cycle. We investigated the possibility that MHV subgenomic mRNA transcription is mediated through a genomic-length RNA template. The results indicate that this is indeed the case, at least early in the infection. Thus, the templates for MHV subgenomic mRNA synthesis may include both genomic- and subgenomic-size RNAs, with the genomic-size RNA being the major template early in infection. Several models of transcription are discussed.

MATERIALS AND METHODS

Virus and cells. MHV strain A59 was propagated once in 17CL1 cells (35), and the culture medium harvested at 18 h postinfection (p.i.) was used as the stock virus throughout the experiments. UV irradiation and RNA labeling experiments were performed in DBT cells (8). The defective interfering (DI) RNA transfection experiments were performed in L2 cells (22).

UV irradiation of virus-infected cells. Six 60-mm-diameter plates of DBT cells were inoculated with A59 at multiplicity of infection of 10 simultaneously (designated 0 h p.i.). After 1 h of virus adsorption, the inoculum was removed and replaced with different types of media as outlined in Fig. 1. At specified time points p.i., medium was removed and cells

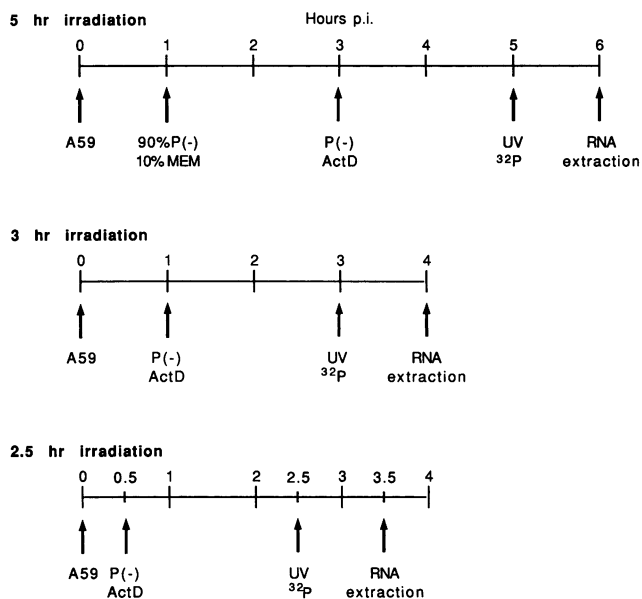


FIG. 1. Schema of experimental schedule. Arrows indicate time points when different procedures were performed. P(-), phosphate-free medium; ActD, actinomycin D; ³²P, ³²P_i.

were washed with phosphate-buffered saline (PBS) at room temperature. After removal of PBS, plates were covered with the plastic lid and a sheet of Whatman 3MM paper and placed at a distance of 50 cm from a 30-W germicidal lamp. One plate was used as a control and was not exposed to UV light. For the remaining five plates, the lids and 3MM papers were removed for 15 s, 30 s, 1 min, 2 min, or 4 min, respectively, for UV exposure and replaced immediately. After UV irradiation, cells were labeled with ³²P_i for 1 h. Each experiment was repeated at least three times to confirm the reproducibility of the results.

Intracellular RNA labeling and extraction. Confluent DBT cells in 60-mm-diameter plates were washed once with minimum essential medium (MEM; Irvine Scientific, Irvine, Calif.) and infected with virus as described above. After 1 h of virus adsorption, inoculum was removed and replaced with 5 ml of phosphate-free medium (0.12 M NaCl, 1 mM sodium citrate, 5 mM KCl, 0.8 mM magnesium sulfate, 1.8 mM CaCl₂, 5.5 mM glucose) containing 10% normal MEM. At 2 h prior to UV irradiation, the media were replaced with 3 ml of 100% phosphate-free medium containing 2.5 μg of actinomycin D (Sigma) per ml. After UV irradiation, 1.2 mCi of ³²P_i (ICN) was immediately added to each plate, and cells were incubated at 37°C for 1 h. After ³²P labeling, plates were placed on ice and rinsed with ice-cold PBS three times. Cells were scraped into 1 ml of PBS with a rubber policeman. After brief centrifugation, cell pellets were dissolved in NTE (0.1 M NaCl, 0.01 M Tris-HCl [pH 7.2], and 1 mM EDTA) containing 0.5% Nonidet P-40 and incubated at 4°C for 10 min. Nuclei were removed by centrifugation, and the supernatant was incubated with an equal volume of 2× proteinase K buffer (0.2 M Tris-HCl [pH 7.5], 25 mM EDTA, 0.3 M NaCl, 2% sodium dodecyl sulfate [SDS]) and 0.4 mg of proteinase K (Boehringer Mannheim) per ml at 37°C for 1 h. RNA was extracted with phenol and chloroform and precipitated with ethanol at -70°C. RNA from each 60-mm-diameter plate was redissolved in 10 to 20 μl of H₂O, and 3

μ l of each sample was used for agarose gel electrophoresis as described previously (25).

Purification of poly(A)-containing RNA. 32 P-labeled RNA extracted as described above was denatured at 94°C for 2 min and diluted into 1 ml of 1 \times binding buffer (0.01 M Tris-HCl [pH 7.5], 0.5 M NaCl, 0.5% SDS, and 1 mM EDTA). RNA was passed three times through a column containing 25 mg of oligo(dT)-cellulose (Collaborative Research Inc., Bedford, Mass.) equilibrated with the binding buffer. Poly(A)-containing RNA was eluted with the elution buffer (0.01 M Tris-HCl [pH 7.5], 0.05% SDS, 1 mM EDTA) as recommended by the manufacturer. Both poly(A)⁺ and poly(A)⁻ RNA fractions were collected by ethanol precipitation. Poly(A)⁻ fractions were used to assess the integrity of RNA.

In vitro transcription of DIssE RNA. DIssE RNA (described in reference 22) was transcribed from the cDNA clone of DIssE RNA in pT7 vector (22), which was linearized with *Xba*I, and transcribed by T7 RNA polymerase (Promega Co., Madison, Wis.) in the presence of a cap analog [7mG(5')ppp(5')G; New England Biolabs, Beverly, Mass.] according to the procedure recommended by the manufacturer (Promega). The reaction mixture was treated with DNase I (2 U; Promega) for 20 min at 37°C, and the product was analyzed by agarose gel electrophoresis. The RNA was ethanol precipitated twice with 2 M ammonium acetate in the presence of glycogen.

RNA transfection. The procedure for RNA transfection was essentially as described previously (21). Briefly, confluent L2 cells grown in 60-mm-diameter plates were infected with A59 at a multiplicity of infection of approximately 5. After 1 h of virus adsorption, the inoculum was removed, and 1 μ g of in vitro-transcribed DIssE RNA in 200 μ l of transfection buffer (600 μ g of DEAE-dextran per ml, 0.14 M LiCl, HEPES [N-2-hydroxyethylpiperazine-N'-2-ethanesulfonic acid; pH 7.5], 1 mM MgCl₂) was added, and the mixture was incubated for 30 min at 37°C. Cells were then washed once with prewarmed MEM and incubated with 4 ml of MEM containing 5% fetal bovine serum at 37°C for 13 h. The culture supernatant, designated P0, was passaged once in DBT cells to increase virus titer. The supernatant from this culture, designated P1, was used for UV irradiation and RNA labeling experiments.

Agarose gel electrophoresis of RNA. RNA samples were denatured with 1 M glyoxal at 50°C for 1 h and then electrophoresed on a 1.0% agarose gel (SeaKem; FMC BioProducts, Rockland, Maine) in 10 mM sodium phosphate buffer as described previously (25).

Quantitation of radioactivity of 32 P-labeled RNAs. After electrophoresis, agarose gels were dried and directly analyzed by the Ambis imaging system (Ambis, San Diego, Calif.) or, alternatively, exposed to X-ray films which were subsequently analyzed with a densitometer. The values obtained for each RNA species were subjected to linear regression analysis.

RNA dot blot analysis. Total cytoplasmic RNA was isolated at various time points p.i. Five micrograms of each sample was heat denatured and spotted on a nitrocellulose membrane (Highbond-C extra; Amersham Corp., Arlington Heights, Ill.) which had been pretreated with 6 \times SSC (0.9 M NaCl, 0.09 M sodium citrate [pH 7.0]). After baking at 80°C for 2 h, the membrane was prehybridized at 55°C for 4 h in a buffer containing 50% formamide, 0.6 M NaCl, 0.06 M sodium citrate, 100 mM sodium phosphate, 50 mM Tris-HCl (pH 7.1), 8 \times Denhardt's reagent without bovine serum albumin (0.16% Ficoll 400, 0.16% polyvinylpyrrolidone [mo-

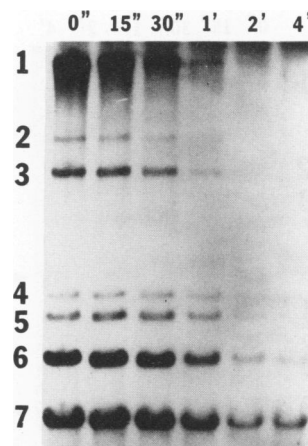


FIG. 2. Effects of UV irradiation at 5 h p.i. on mRNA synthesis. A59-infected cells were exposed to UV light at 5 h p.i. for various lengths of time as indicated (in seconds ['] or minutes ['']) above the lanes. Cells were labeled with 32 P_i immediately for 1 h, and the cytoplasmic RNA was extracted. The RNA was denatured by glyoxal and subjected to gel electrophoresis. Each lane contained approximately one-seventh of the total RNA from one 60-mm-diameter plate. The seven viral mRNAs are numbered 1 to 7.

lecular weight, 360,000)), 0.1% SDS, 0.05 mg of tRNA per ml, and 0.5 mg of salmon sperm DNA per ml. The membrane was then hybridized overnight with the same solution containing 32 P-labeled RNA probe and 17% dextran sulfate. RNA probes used in this study were transcribed from cDNA clones representing the entire gene 7 (1.7 kb), including the upstream intergenic sequence and poly(A) tail, in either negative or positive sense. The RNA probes were prepared by in vitro transcription, using T7 RNA polymerase in the presence of [α - 32 P]UTP (ICN) according to the procedure recommended by the manufacturer (Promega). After precipitation twice with ammonium acetate, the 32 P-labeled probe (10⁸ cpm/ μ g of template DNA) was used directly for hybridization. After hybridization, the membrane was washed four times for 5 min each at room temperature, two times for 20 min each at 70°C with 2 \times SSC-0.1% SDS, and two times for 20 min each at 70°C with 0.1 \times SSC-0.1% SDS. The specificity of hybridization was monitored by hybridization of either probe to in vitro-transcribed positive- or negative-sense unlabeled RNA (10 and 100 μ g) from the same cDNA clones used to make the RNA probes.

RESULTS

Effects of UV irradiation on mRNA synthesis at late time points p.i. To determine the UV sensitivity of mRNA synthesis in MHV-infected cells at different time points of infection, we first repeated the experiment published previously (10, 34), which demonstrated that the UV target size of each mRNA was proportional to its physical size. We first irradiated A59-infected cells with increasing doses of UV light at 5 h p.i., when viral RNA synthesis was most active, and examined viral RNA synthesis by labeling with 32 P_i. The 32 P-labeled viral RNA was then examined by agarose gel electrophoresis. As shown in Fig. 2, the sensitivity of different viral mRNA species to UV irradiation roughly paralleled the size of each mRNA; i.e., the smaller the mRNA, the more resistant it was. This finding agreed with the published results (10, 34) and suggested that the UV

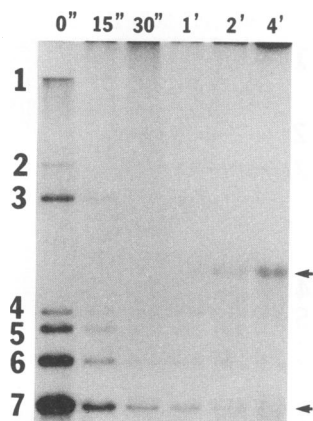


FIG. 3. Effects of UV irradiation at 2.5 h p.i. on mRNA synthesis. A59-infected cells were exposed to UV at 2.5 h p.i. for various lengths of time (indicated in seconds ['] or minutes [']) and ^{32}P labeled immediately. The poly(A)-containing RNA fraction was applied to gel electrophoresis. Each lane contained the entire poly(A) $^{+}$ fraction from a 60-mm-diameter plate. The 28S and 18S rRNAs are indicated.

target sizes of the templates for different mRNA species were the same as their physical sizes. This result was consistent with the interpretation that the viral subgenomic mRNAs were synthesized either directly from their corresponding subgenomic negative-stranded RNA counterparts (28–30) or by a discontinuous transcription process, such as leader-primed transcription, from a full-length RNA template (4, 11).

Effects of UV irradiation on mRNA synthesis at early time points p.i. To critically address the primary mechanism of synthesis of MHV mRNAs, we studied the UV inactivation kinetics of RNA synthesis early in the infection. We first carried out a preliminary study to determine the earliest time when viral RNA synthesis could be detected by radioisotope labeling. It was found that 2.5 h p.i. was the earliest time point at which ^{32}P labeling of RNA could give clearly distinguishable and reproducible viral mRNA patterns (data not shown). Although a small amount of ^{32}P -labeled RNA could be detected as early as 2 h p.i., the intensity of the labeled viral RNA was not strong enough to allow reliable quantitation of different viral RNA species. Hence, we studied UV sensitivity of MHV mRNA synthesis at 2.5 h p.i. The A59-infected DBT cells were irradiated with different doses of UV light at 2.5 h p.i. and immediately labeled with ^{32}P for 1 h. Preliminary studies showed that there was a high background of cellular RNA synthesis, even in the presence of actinomycin D. Thus, the RNA samples were poly(A) selected, and the poly(A) $^{+}$ fractions were used for agarose gel electrophoresis. In contrast to the virus-infected cells irradiated at 5 h p.i. (Fig. 2), a drastic decrease in the amount of every viral mRNA species was evident after short UV exposure: the synthesis of every viral mRNA species decreased by more than 80% after only 15 s of UV irradiation (Fig. 3). The extent of inhibition was approximately the same for all of the mRNAs. However, the residual portions of the smaller mRNAs (e.g., mRNAs 6 and 7) remaining after 15 s of UV irradiation decreased more gradually than the remaining larger mRNAs did after additional UV irradiation. The rate of this latter decrease for each mRNA was proportional to its RNA size. This result suggested that at this early time point, the majority of each mRNA has a UV target size much

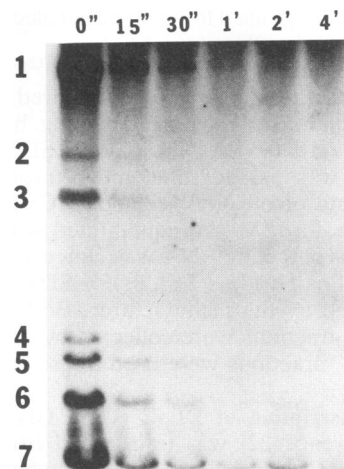


FIG. 4. Effects of UV irradiation at 3 h p.i. on mRNA synthesis. A59-infected cells were UV irradiated at 3 h p.i. and ^{32}P labeled immediately. Each lane contained approximately one-third of the total RNA from a 60-mm-diameter plate.

bigger than its RNA size, but a small portion of each mRNA has a target size equivalent to the size of the RNA. Thus, viral mRNA synthesis may require two different types of templates: the major one is the genomic-length template, and the other one comprises the subgenomic-size templates. Figure 3 also shows that the 28S and 18S rRNAs were detectable in samples irradiated for 2 and 4 min, in which the viral RNA synthesis was almost completely inhibited. The reason for the detection of these RNAs is not clear.

We next examined the UV sensitivity of viral mRNA synthesis at 3 h p.i. At this time point, the background cellular RNA synthesis was minimal so that viral RNA was directly examined without poly(A) selection. The results were similar to those obtained at 2.5 h p.i. A small UV dose (15-s exposure) inhibited the synthesis of every mRNA to the same extent (80%), while the remaining mRNAs were inhibited by increasing UV doses at the different rates proportional to their RNA sizes (Fig. 4). These results confirmed the conclusion that at early time points in MHV infection, there are two different templates for subgenomic mRNA synthesis.

To determine the precise rate of UV inactivation of viral mRNAs, we performed quantitative analysis of the ^{32}P -labeled viral mRNAs synthesized after being irradiated at different time points p.i. (Fig. 5). The results were derived from linear regression analysis of the data obtained by densitometric readings of RNA bands on the electropherograms and also by direct measurement of radioactivity of each RNA species on the gels. Figure 5 shows that at 5 h p.i., UV sensitivity of each mRNA was directly proportional to the size of the mRNAs. In contrast, at 2.5 or 3 h p.i., a vast majority (approximately 80%) of every mRNA species showed very high sensitivity equivalent to that of the genomic RNA, but small amounts of mRNAs 5 to 7 had lower UV sensitivities which were proportional to their RNA sizes. The quantities of mRNAs 1 to 4 at higher UV doses could not be analyzed because of low radioactivity. These results strongly suggested that the majority of viral subgenomic mRNAs have a genomic-length UV target size early in the infection.

To determine whether the viral RNA synthesis observed at early time points represented positive- or negative-

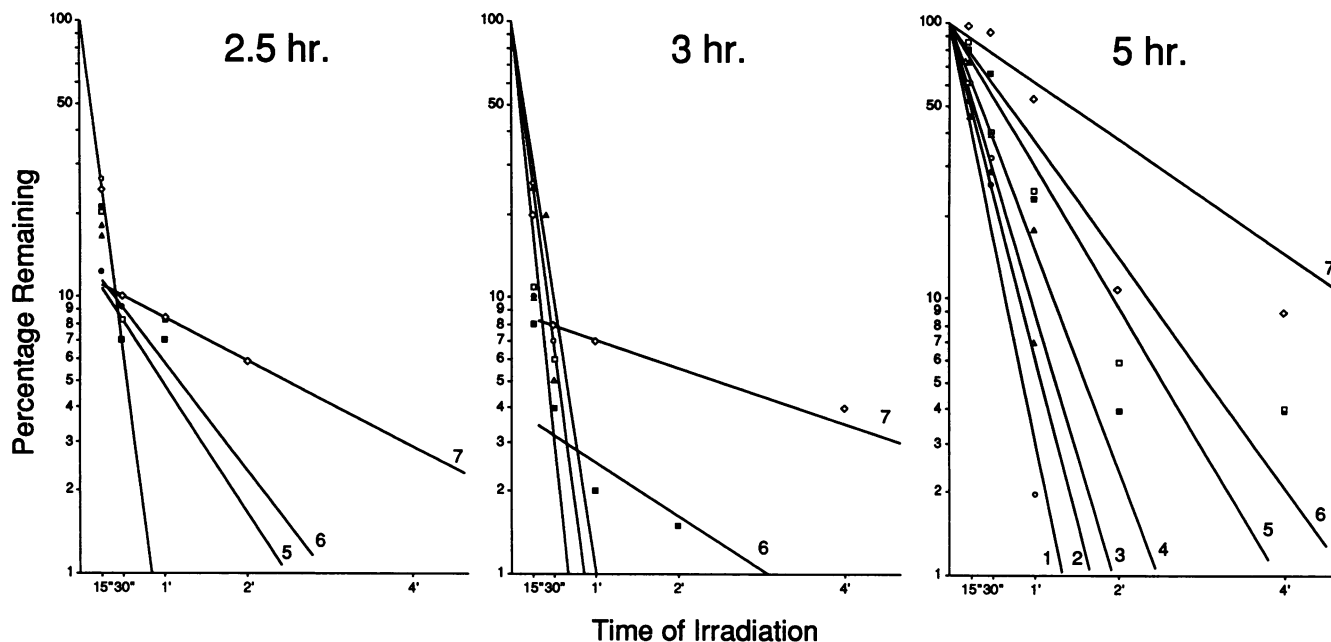


FIG. 5. Comparison of UV inactivation kinetics at different time points p.i. The graphs were drawn on the basis of computer-generated linear regression analysis of at least three independent experiments. Data are for mRNAs 1 (\circ), 2 (\bullet), 3 (Δ), 4 (\blacktriangle), 5 (\square), 6 (\blacksquare), and 7 (\diamond). ", seconds; ', minutes.

stranded RNA, dot blot hybridization of intracellular RNA extracted at different time points p.i. was performed. We used *in vitro*-transcribed sense and antisense gene 7 RNAs as probes, which hybridize to all of the viral RNA species of complementary sense because of the nested-set structure of MHV RNAs (13, 17). Figure 6 shows that positive-stranded RNA was in large excess over negative-stranded RNA throughout the infection, even at the earliest time point (3 h p.i.) when viral RNA began to be detectable. The amount of negative-stranded RNA constituted less than 1% of the total viral RNA and was not detectable by this method at early time points (before 4 h p.i.). These data indicated that even very early in infection, RNA synthesis measured by radiolabeling of RNA represented mainly positive-stranded

RNAs. Thus, UV sensitivity of RNA synthesis measured in this study most likely reflected the target size of the template for positive-stranded mRNAs.

Effects of UV irradiation on DI RNA synthesis early in the infection. Since virus-specific RNA polymerase, which is synthesized from the genome-size mRNA 1 (15, 26), is needed for viral RNA synthesis, it is possible that the large UV target size of mRNA synthesis early in the infection could be due to inhibition of the synthesis of RNA polymerase. If this was the case, the UV target size of mRNAs measured in this study would not reflect the size of RNA template for viral mRNAs. To rule out this possibility, we studied the UV sensitivity of a DI RNA, DIssE (22), which depended on RNA polymerase synthesized by the helper virus for replication and yet replicated on an RNA template of its own size (2.2 kb) (21, 22). Thus, if the effects of UV irradiation on viral mRNA synthesis early in infection were due to deprivation of viral RNA polymerase, DI RNA synthesis would be inhibited to the same extent as synthesis of all of the viral mRNAs. We first prepared DIssE-containing A59 by transfecting *in vitro*-transcribed DIssE RNA into A59-infected cells. The virus harvested was amplified by an additional passage in DBT cells to increase the amount of DIssE RNA as described previously (21, 22). The UV sensitivity of DI RNA synthesis was then studied at 3 h p.i., using this virus stock. Figure 7A shows that the viral mRNA synthesis was not interfered with by DIssE RNA under this condition, in agreement with the previous studies (21, 22). Similar to results shown in Fig. 4, syntheses of all of the viral mRNAs were significantly inhibited by a small UV dose (15-s irradiation). In contrast, DIssE RNA synthesis was much more resistant to UV inactivation. Most notably, DIssE RNA synthesis was more UV resistant than mRNA 7 synthesis, even though DIssE (2.2 kb) was larger than mRNA 7 (1.7 kb). The UV inactivation kinetic graphs based on linear regression analysis (Fig. 7B) showed that the

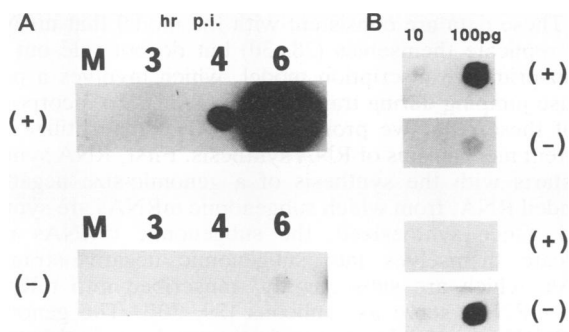


FIG. 6. Dot blot analysis of positive- and negative-stranded A59 RNA in total cytoplasmic RNA. Total cytoplasmic RNA was extracted at various time points p.i. from A59-infected cells and hybridized with *in vitro*-transcribed ^{32}P -labeled sense or antisense RNA of A59 gene 7 (A). Lane M, mock-infected cellular RNA. The specificity and sensitivity of the probes used were determined by hybridization to the determined amounts of the unlabeled *in vitro*-transcribed RNA from the same plasmids (B).

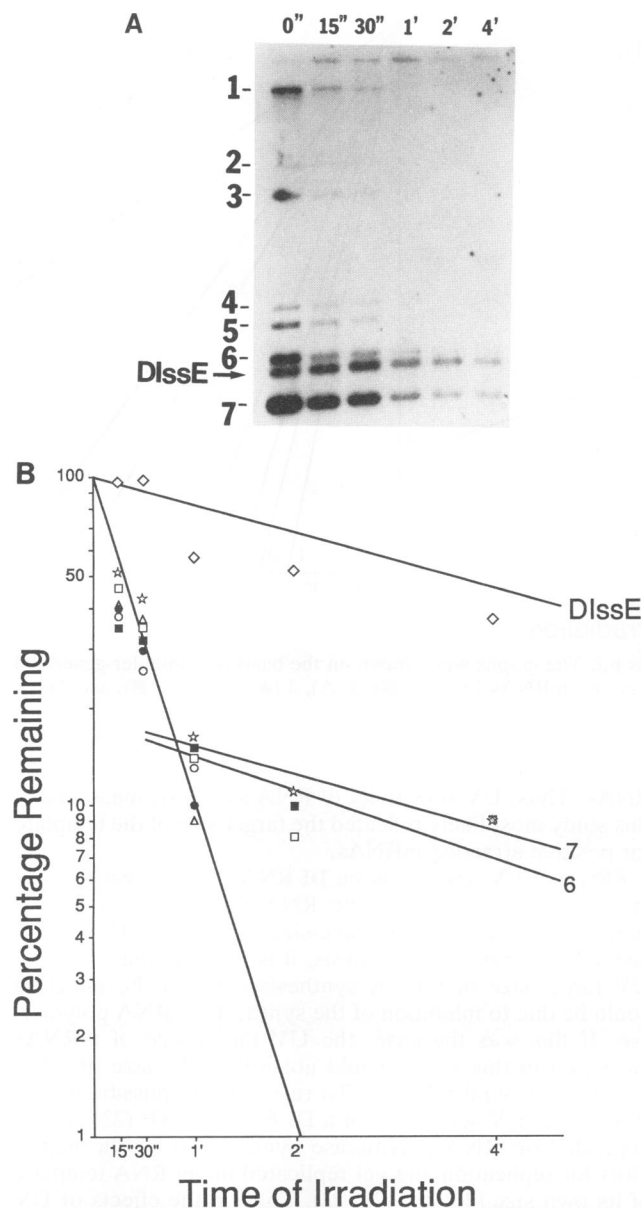


FIG. 7. Effects of UV irradiation on DIssE RNA synthesis early in infection. (A) UV irradiation of cells infected with DIssE-containing A59 virus at 3 h p.i. Cells were ^{32}P labeled immediately after irradiation for 1 h. RNA was poly(A) selected and subjected to gel electrophoresis after denaturation. (B) UV inactivation kinetics of A59-specific and DIssE RNAs. The graph was based on the linear regression analysis of two separate experiments as described for Fig. 4. Data are for DIssE (\diamond) RNA and mRNAs 1 (\circ), 2 (\bullet), 3 (Δ), 4 (\blacktriangle), 5 (\square), 6 (\blacksquare), and 7 (\ast). ", seconds; ', minutes.

majority of every mRNA species had a high UV sensitivity equivalent to that of the genomic-size RNA, but the remaining mRNAs 6 and 7 had a much lower UV sensitivity which was in proportion to their RNA size at higher doses of UV. This result agreed with the findings in Fig. 4 and 5. In contrast, DIssE showed single UV inactivation kinetics, which indicated a UV target size equivalent to its physical size (2.2 kb). This difference in the UV sensitivity between DIssE RNA and viral mRNAs suggested strongly that the

large UV target size of A59 mRNAs early in infection was not caused by a deficiency of RNA polymerase and/or other protein products but rather reflected the true size of the template for subgenomic mRNA synthesis.

DISCUSSION

Results shown previously (10, 34) and in this report indicated that late in MHV infection, UV target sizes of MHV subgenomic RNAs correspond to their physical sizes. Furthermore, this study revealed that early in infection, MHV mRNA species can be divided into two components in terms of UV sensitivity: the majority of every mRNA species had a UV target size similar to that of the genomic RNA, while a small population of subgenomic mRNAs demonstrated a higher resistance to UV inactivation, with a UV target size equivalent to its RNA size. This finding suggests that transcription of the majority of subgenomic mRNAs of MHV requires the synthesis of a full-length genomic RNA early in the infection. This genomic-length RNA is probably required as the template for mRNA transcription rather than as an mRNA for the translation of polymerase. The latter conclusion was supported by the finding that a DI RNA, which utilizes RNA polymerase synthesized from the helper virus RNA, had a UV target size smaller than that of even the smallest mRNA (mRNA 7) early in infection. Thus, RNA polymerase was not the limiting factor under the conditions studied. These results strongly suggest that the synthesis of the subgenomic mRNAs of MHV requires a genomic-size template at least early in the infection. We do not know the origin of the minor components of mRNAs which had UV target sizes corresponding to their RNA sizes early in infection. They could be derived directly from the replication of mRNAs nonspecifically packaged into the virus particles (29), or they may be amplified from the mRNAs transcribed from the genomic-length template. Although the UV sensitivity of mRNAs could not be examined at an even earlier time point because of low amounts of radioactivity, our results nevertheless indicated the presence of a primary mechanism of transcription of subgenomic mRNAs from the genomic-length template early in infection.

The subgenomic sizes of UV targets for the MHV mRNAs late in the infection correlated with the detection of subgenomic replicative intermediate RNAs (28) and subgenomic negative-stranded RNAs in coronavirus-infected cells (9, 29, 30). These data are consistent with the model that mRNAs may replicate themselves (28, 30) but do not rule out the leader-primed transcription model, which involves a polymerase jumping during transcription (4, 11). To incorporate all of these data, we propose that MHV may utilize two different mechanisms of RNA synthesis. First, RNA synthesis starts with the synthesis of a genomic-size negative-stranded RNA, from which subgenomic mRNAs are synthesized. Once synthesized, the subgenomic mRNAs may replicate themselves into subgenomic negative-stranded RNAs, which are subsequently transcribed into mRNAs (i.e., mRNAs serve as replicons [29, 30]). The genomic-length RNA required early in infection as shown in this study could represent either a precursor RNA, which is processed by an RNA splicing mechanism to form negative-stranded subgenomic RNAs, or a genomic-size template RNA, which is used for the synthesis of subgenomic mRNAs by a discontinuous transcription mechanism, such as leader-primed transcription (11). These two possibilities cannot be rigorously distinguished at the present time. However, we

consider the first possibility less likely, since it necessitates invoking a new kind of RNA splicing mechanism which occurs in cytoplasm and utilizes a novel splicing sequence motif. The second possibility is more compatible with the existing data, which suggest a discontinuous nature of MHV RNA transcription involving a free leader RNA species (see the introduction and reference 11). Although there is no direct experimental evidence that mRNAs can be replicated, replication seems probable considering that the subgenomic mRNAs and genomic RNA have identical sequences at both the 5' and 3' ends. If this is indeed the case, the minor amounts of mRNAs nonspecifically packaged in the virus particles should be able to serve as templates for mRNA replication (29, 30), consistent with the small amount of mRNAs which had subgenomic UV target size early in infection. However, (i) the fact that we have not detected significant amounts of subgenomic mRNAs in MHV particles (data not shown) and (ii) the requirement for a genomic RNA template shown in this study argue that this pathway is not the major mechanism of mRNA synthesis early in infection. Furthermore, Makino et al. showed that an in vitro-transcribed DI RNA containing an intergenic sequence can synthesize a subgenomic mRNA in MHV-infected cells, suggesting that the subgenomic mRNA can be transcribed from the full-length template (18). Also, an in vitro transcription system prepared from the MHV-infected cells late in the infection could utilize an exogenous leader RNA for mRNA transcription (2). These results suggest that the proposed first mechanism of subgenomic mRNA transcription from the full-length template may persist throughout the entire viral replication cycle. It should be pointed out that the detection of subgenomic negative-stranded RNAs did not rule out the model of discontinuous transcription during positive-stranded RNA synthesis late in infection, since the leader priming may take place on negative-stranded subgenomic templates.

One additional possibility should be considered: the discontinuous transcription mechanism may occur during negative-stranded RNA synthesis by a polymerase jumping mechanism. In this scenario, the early requirement for the full-length RNA will be for the synthesis of genomic RNA template for subsequent subgenomic negative-stranded RNA synthesis. This mechanism, however, is inconsistent with the observation that the transcriptions of several subgenomic mRNAs are regulated by the leader RNA sequences (14, 19, 31). If polymerase jumping took place during negative-stranded RNA synthesis, it would be difficult for the leader to regulate transcription of these mRNAs, since the antileader RNA is located on the downstream side of the subgenomic negative-stranded RNAs. Thus, we favor the leader-primed transcription model, at least early in infection. In this model, the leader RNA is located upstream of the viral genes, making it possible for the leader to regulate the transcription of the subgenomic mRNAs.

The results presented here also indicated that the amount of negative-stranded RNA made by MHV was much lower than that detected in other studies (27, 30). The reason for this discrepancy is not clear. However, the negative-stranded RNA continued to increase until late in the infection. This finding is more consistent with the observation made by Sawicki and Sawicki that negative-stranded RNA synthesis peaked at 5 h p.i. in MHV-infected cells (27) and does not agree with the data obtained from the analysis of MHV polymerase activity which indicated that the negative-stranded RNA synthesis peaked at earlier time points (6).

Another puzzling observation is that at early time points

p.i., rRNA synthesis increased when MHV mRNA synthesis was inhibited by higher UV doses (Fig. 3). The rRNA was detected even after a single round of poly(A) selection of RNA. This finding suggests that MHV may encode some early functions which can inhibit RNA synthesis. It is also possible that UV induces expression of some gene(s) necessary for rRNA synthesis. This issue remains to be studied.

ACKNOWLEDGMENTS

We thank Tom Macnaughton for the dot blot procedure.

This work was supported by Public Health Service research grant AI 19244 from the National Institutes of Health. L.R.B. was supported in part by a Feiger predoctoral fellowship from the Norris Cancer Center, University of Southern California. K.Y. is a research associate and M.M.C.L. is an investigator of the Howard Hughes Medical Institute.

REFERENCES

1. Abraham, G., and A. K. Banerjee. 1976. Sequential transcription of the genes of vesicular stomatitis virus. *Proc. Natl. Acad. Sci. USA* 73:1504-1508.
2. Baker, S. C., and M. M. C. Lai. 1990. An in vitro system for the leader-primed transcription of coronavirus mRNAs. *EMBO J.* 9:4173-4179.
3. Ball, L. A., and C. N. White. 1976. Order of transcription of genes of vesicular stomatitis virus. *Proc. Natl. Acad. Sci. USA* 73:442-446.
4. Baric, R. S., S. A. Stohlman, and M. M. C. Lai. 1983. Characterization of replicative intermediate RNA of mouse hepatitis virus: presence of leader RNA sequences on nascent chains. *J. Virol.* 48:633-640.
5. Baric, R. S., S. A. Stohlman, M. K. Razavi, and M. M. C. Lai. 1985. Characterization of leader-related small RNAs in coronavirus-infected cells: further evidence for leader-primed mechanism of transcription. *Virus Res.* 3:19-33.
6. Brayton, P. R., S. A. Stohlman, and M. M. C. Lai. 1984. Further characterization of mouse hepatitis virus RNA-dependent RNA polymerases. *Virology* 133:197-201.
7. Glazier, K., R. Raghow, and D. W. Kingsbury. 1977. Regulation of Sendai virus transcription: evidence for a single promoter in vivo. *J. Virol.* 21:863-871.
8. Hirano, N., K. Fujiwara, S. Hino, and M. Matsumoto. 1974. Replication and plaque formation of mouse hepatitis virus (MHV-2) in mouse cell line DBT cell culture. *Arch. Gesamte Virusforsch.* 44:298-302.
9. Hofmann, M. A., P. B. Sethna, and D. A. Brian. 1990. Bovine coronavirus mRNA replication continues throughout persistent infection in cell culture. *J. Virol.* 64:4108-4114.
10. Jacobs, L., W. J. M. Spaan, M. C. Horzinek, and B. A. M. van der Zeijst. 1981. The synthesis of the subgenomic mRNAs of mouse hepatitis virus is initiated independently: evidence from UV transcription mapping. *J. Virol.* 39:401-406.
11. Lai, M. M. C. 1990. Coronavirus: organization, replication and expression of genome. *Annu. Rev. Microbiol.* 44:303-333.
12. Lai, M. M. C., R. S. Baric, P. R. Brayton, and S. A. Stohlman. 1984. Characterization of leader RNA sequences on the virion and mRNAs of mouse hepatitis virus, a cytoplasmic RNA virus. *Proc. Natl. Acad. Sci. USA* 81:3626-3630.
13. Lai, M. M. C., P. R. Brayton, R. C. Armen, C. D. Patton, C. Pugh, and S. A. Stohlman. 1981. Mouse hepatitis virus A59: mRNA structure and genetic localization of the sequence divergence from hepatotropic strain MHV-3. *J. Virol.* 39:823-834.
14. La Monica, N., K. Yokomori, and M. M. C. Lai. 1992. Coronavirus mRNA synthesis: identification of novel transcription initiation signals which are differentially regulated by different leader sequences. *Virology* 188:402-407.
15. Lee, H.-J., C.-K. Shieh, A. E. Gorbalenya, E. V. Koonin, N. La Monica, J. Tuler, A. Bagdzhadzhyan, and M. M. C. Lai. 1991. The complete sequence (22 kilobases) of murine coronavirus gene 1 encoding the putative proteases and RNA polymerase.

- Virology **180**:567–582.
16. Leibowitz, J. L., S. R. Weiss, E. Paavola, and C. W. Bond. 1982. Cell-free translation of murine coronavirus RNA. *J. Virol.* **43**:905–913.
 17. Leibowitz, J. L., K. C. Wilhelmsen, and C. W. Bond. 1981. The virus-specific intracellular RNA species of two murine coronaviruses: MHV-A59 and MHV-JHM. *Virology* **114**:39–51.
 18. Makino, S., M. Joo, and J. K. Makino. 1991. A system for study of coronavirus mRNA synthesis: a regulated, expressed subgenomic defective interfering RNA results from intergenic site insertion. *J. Virol.* **65**:6031–6041.
 19. Makino, S., and M. M. C. Lai. 1989. Evolution of the 5'-end of genomic RNA of murine coronaviruses during passages in vitro. *Virology* **169**:227–232.
 20. Makino, S., and M. M. C. Lai. 1989. High-frequency leader sequence switching during coronavirus defective interfering RNA replication. *J. Virol.* **63**:5285–5292.
 21. Makino, S., C.-K. Shieh, J. G. Keck, and M. M. C. Lai. 1988. Defective interfering particles of murine coronavirus: mechanism of transcription of defective viral RNA. *Virology* **163**:104–111.
 22. Makino, S., C.-K. Shieh, L. H. Soe, S. C. Baker, and M. M. C. Lai. 1988. Primary structure and translation of a defective interfering RNA of murine coronavirus. *Virology* **166**:550–560.
 23. Makino, S., L. H. Soe, C.-K. Shieh, and M. M. C. Lai. 1988. Discontinuous transcription generates heterogeneity at the leader fusion sites of coronavirus mRNAs. *J. Virol.* **62**:3870–3873.
 24. Makino, S., S. A. Stohlman, and M. M. C. Lai. 1986. Leader sequences of murine coronavirus mRNAs can be freely reassorted: evidence for the role of free leader RNA in transcription. *Proc. Natl. Acad. Sci. USA* **83**:4204–4208.
 25. Makino, S., F. Taguchi, N. Hirano, and K. Fujiwara. 1984. Analysis of genomic and intracellular viral RNAs of small plaque mutants of mouse hepatitis virus, JHM strain. *Virology* **139**:138–151.
 26. Pachuk, C. J., P. J. Bredenbeek, P. W. Zoltick, W. J. M. Spaan, and S. R. Weiss. 1989. Molecular cloning of the gene encoding the putative polymerase of mouse hepatitis coronavirus strain A59. *Virology* **171**:141–148.
 27. Sawicki, S. G., and D. L. Sawicki. 1986. Coronavirus minus-strand RNA synthesis and effect of cycloheximide on coronavirus RNA synthesis. *J. Virol.* **57**:328–334.
 28. Sawicki, S. G., and D. L. Sawicki. 1990. Coronavirus transcription: subgenomic mouse hepatitis virus replicative intermediates function in RNA synthesis. *J. Virol.* **64**:1050–1056.
 29. Sethna, P. B., M. A. Hofmann, and D. A. Brian. 1991. Minus-strand copies of replicating coronavirus mRNAs contain anti-leaders. *J. Virol.* **65**:320–325.
 30. Sethna, P. B., S.-L. Hung, and D. A. Brian. 1989. Coronavirus subgenomic minus-strand RNAs and the potential for mRNA replicons. *Proc. Natl. Acad. Sci. USA* **86**:5626–5630.
 31. Shieh, C.-K., H.-J. Lee, K. Yokomori, N. La Monica, S. Makino, and M. M. C. Lai. 1989. Identification of a new transcription initiation site and the corresponding functional gene 2b in the murine coronavirus RNA genome. *J. Virol.* **63**:3729–3736.
 32. Shieh, C.-K., L.-H. Soe, S. Makino, M.-F. Chang, S. A. Stohlman, and M. M. C. Lai. 1987. The 5'-end sequence of the murine coronavirus genome: implications for multiple fusion sites in the leader-primed transcription. *Virology* **156**:321–330.
 33. Spaan, W., H. Delius, M. Skinner, J. Armstrong, P. Rottier, S. Smeekens, B. A. M. van der Zeijst, and S. G. Siddell. 1983. Coronavirus mRNA synthesis involves fusion of noncontiguous sequences. *EMBO J.* **2**:1839–1844.
 34. Stern, D. F., and B. M. Sefton. 1982. Synthesis of coronavirus mRNAs: kinetics of inactivation of infectious bronchitis virus RNA synthesis by UV light. *J. Virol.* **42**:755–759.
 35. Sturman, L. S., and K. K. Takemoto. 1972. Enhanced growth of a murine coronavirus in transformed mouse cells. *Infect. Immun.* **6**:501–507.